Grafting of Organoruthenium Oligomers on Quartz Substrates: Synthesis, Electrochemistry, Optical Properties, and AFM Investigations

Mathieu J.-L. Tschan,[†] Younes Makoudi,[‡] Frédéric Chérioux,*[,‡] Frank Palmino,[‡] Isabelle Fabre-Francke,[§,||] Saïd Sadki,[||] and Georg Süss-Fink[†]

Institut de Chimie, Université de Neuchâtel, Case Postale 158, CH-2009 Neuchâtel, Switzerland, Laboratoire FEMTO-ST, UMR CNRS 6174, Université de Franche-Comté, 32 Avenue de l'Observatoire, F-25044 Besançon Cedex, France, CEA-LETI-MINATEC, 17 Rue des Martyrs, F-38054 Grenoble Cedex 09, France, and UMR SPraM (CEA, CNRS, UJF), DRFMC CEA de Grenoble, 17 Rue des Martyrs, F-38054 Grenoble Cedex 09, France

Received April 2, 2007. Revised Manuscript Received May 23, 2007

A new type of organometallic oligomers has been obtained from the reaction of $[(C_6Me_6)_2Ru_2H_3]^+$ and dithiophenol derivatives. These oligomers are highly ordered because of the steric hindrance around the metal center and the rigidity of the aromatic units. The electrochemical behavior of the monomers and the oligomers has been studied both in reduction and in oxidation modes. The oligomers have been grafted via electrostatic interactions on glass substrates prefunctionalized by self-assembled monolayers (SAMs). The optical properties of the films have also been investigated.

Introduction

Over the past three decades, arene ruthenium complexes have been extensively studied,[1] one of the driving forces being their catalytic potential.[2] One of the most interesting representatives, the unsaturated dinuclear complex $[(C_6Me_6)_2Ru_2(\mu_2\text{-}H)_3]^+$, which is isolated as the tetrafluoroborate salt[3] and soluble in both water or organic solvents, turned out to be a versatile starting material for organometallic synthesis. Thus, it has been used as a precursor for the assembly of trinuclear arene ruthenium clusters,[4] and as a building block for conjugated organometallic oligomers.[5] At the same time, conjugated organic oligomers and/or polymers have attracted much attention for their electronic and optical properties and, more recently, for possible applications in nanoelectronics and chemosensing.[6] An extended π-conjugated carbon skeleton is the key feature of such materials. The incorporation of transition metals in conducting polymer systems allows us to expand the functioning and ultimate applications of such materials.[7] Thus, there are many reports on the incorporation of redox-active metal centers into the main chain of conducting structures, in order to develop devices for sensing, for solar energy conversion or for catalytic applications. Moreover, electrostatic lattices formed through electrostatic self-assembly of oppositely charged molecules, oligomers, or polymers have been of great interest.[8] The techniques used for the assembly of such materials involve the sequential adsorption of positively and negatively charged compounds from a solution to produce nanostructured mono-

* Corresponding author. Fax: +33 381 853 998, Tel: +33 381 853 951. E-mail: frederic.cherioux@femto-st.fr.
[†] Université de Neuchâtel.
[‡] Université de Franche-Comté.
[§] CEA-LETI-MINATEC.
[||] Université Joseph Fourrier.

(1) (a) Bennett, M. A. *Coord. Chem. Rev.* **1997**, *166*, 225. (b) Meister, G.; Rheinwald, G.; Stoeckli-Evans, H.; Süss-Fink, G. *J. Chem. Soc., Dalton Trans.* **1994**, 3215. (c) Chérioux, F.; Thomas, C. M.; Therrien, B.; Süss-Fink, G. *Chem.—Eur. J.* **2002**, *8*, 4377. (d) Chérioux, F.; Therrien, B.; Süss-Fink, G. *Chem. Commun.* **2004**, 204. (e) Pinto, P.; Marconi, G.; Heinemann, F. W.; Zenneck, U. *Organometallics* **2004**, *23*, 374. (f) Stodt, R.; Gencaslan, S.; Muller, I. M.; Shledrick, W. S. *Eur. J. Inorg. Chem.* **2003**, 1873. (g) Kraemer, R. *Angew. Chem., Int. Ed.* **1996**, *35*, 1197. (h) Pilette, D.; Ouzzine, K.; Le Bozec, H.; Dixneuf, P. H.; Rickard, C. E. F.; Roper, W. R. *Organometallics* **1992**, *11*, 809. (i) Crabtree, R. H.; Pearman, A. J. J. *Organomet. Chem.* **1977**, *141*, 325. (j) Vieille-Petit, L.; Süss-Fink, G.; Therrien, B.; Ward, T. R.; Stoeckli-Evans, H.; Labat, G.; Karmazin-Brelot, L.; Neels, A.; Burgi, T.; Finke, R. G.; Hagen, C. M. *Organometallics* **2005**, *24*, 6104. (k) Süss-Fink, G.; Faure, M.; Ward, T. R. *Angew. Chem., Int. Ed.* **2002**, *41*, 99.

(2) (a) Daguenet, C.; Scopelliti, R.; Dyson, P. J. *Organometallics* **2004**, *23*, 4849. (b) Brandt, P.; Roth, P.; Andersson, P. G. *J. Org. Chem.* **2004**, *69*, 4885. (c) Yamakawa, M.; Yamada, I.; Noyori, R. *Angew. Chem., Int. Ed.* **2001**, *40*, 2818. (d) Noyori, R.; Hashiguchi, S. *Acc. Chem. Res.* **1997**, *30*, 97. (e) Süss-Fink, G. *Synthetic Methods of Organometallic and Inorganic Chemistry*; Georg Thieme Verlag: Stuttgart, Germany, 2001; Vol. 10.

(3) (a) Bennett, M. A.; Huang, T.-N.; Matheson, T. W.; Smith, A. K. *Inorg. Synth.* **1982**, *21*, 74. (b) Jahncke, M.; Meister, G.; Rheinwald, G.; Stoeckli-Evans, H.; Süss-Fink, G. *Organometallics* **1997**, *16*, 1137. (c) Bennett, M. A.; Ennett, P. J. *Inorg. Chim. Acta* **1992**, *198−200*, 583.

(4) (a) Vieille-Petit, L.; Therrien, B.; Süss-Fink, G. *Eur. J. Inorg. Chem.* **2003**, 3707. (b) Vieille-Petit, L.; Therrien, B.; Süss-Fink, G.; Ward, T. *J. Organomet. Chem.* **2003**, *684*, 117. (c) Vieille-Petit, L.; Karmazin-Brelot, L.; Labat, G.; Süss-Fink, G. *Eur. J. Inorg. Chem.* **2004**, *3907*.

(5) Tschan, M. J.-L.; Chérioux, F.; Therrien, B.; Süss-Fink G. *Eur. J. Inorg. Chem.* **2004**, 2405.

(6) (a) Shirakawa, H. *Angew. Chem., Int. Ed.* **2001**, *40*, 2574. (b) MacDiarmid, A. G. *Angew. Chem., Int. Ed.* **2001**, *40*, 2581. (c) Heeger, A. J. *Angew. Chem., Int. Ed.* **2001**, *40*, 2591. (d) Swager, T. M. *Acc. Chem. Res.* **1998**, *31*, 201. (e) Holliday, B. J.; Swager, T. M. *Chem. Commun.* **2005**, 23.

(7) Manners, I. *Synthetic Metal-Containing Polymers*; Wiley-VCH: Weinheim, Germany, 2004.

(8) (a) Decher, G. *Science* **1997**, *277*, 1232. (b) Osman, M. A.; Ernst, M.; Meier, B. H.; Suter, U. W. *J. Phys. Chem. B* **2002**, *106*, 653. (c) Man, K. Y. K.; Wong, H. L.; Chan, W. K.; Djurisic, A. B.; Beach, E.; Rozeveld, S. *Langmuir* **2006**, *22*, 3368.

10.1021/cm070908p CCC: $37.00
Published on Web 06/30/2007

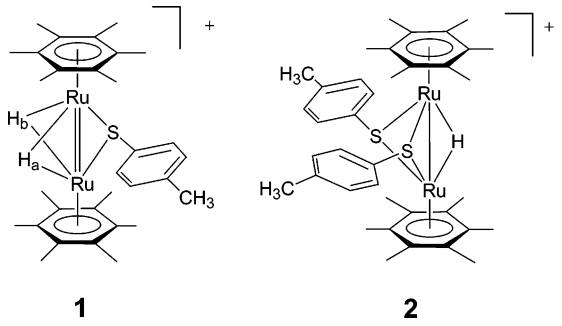

1 **2**

Figure 1. Complexes **1** and **2**.

or multilayer films of controlled thickness. These architectures can be used to achieve unique and tunable physical properties for the development of devices.[9]

In this paper, we report (i) the synthesis of organometallic oligomers obtained from the reaction between the dinuclear arene ruthenium complex $[(C_6Me_6)_2Ru_2H_3]^+$ and dithiophenol derivatives, (ii) the electrochemical behavior of the monomer and the polymers, and (iii) the grafting of these polymers on a functionalized quartz substrate and the investigation of their optical properties as well as AFM imaging of the modified substrate.

Results and Discussion

Recently we found that the organometallic cation $[(C_6Me_6)_2Ru_2H_3]^+$, isolated as the tetrafluoroborate salts,[10] reacts with secondary or tertiary phosphines, PR_2H or PR_3, to give, via P−H or P−C bond cleavage, complexes of the type $[(C_6Me_6)_2Ru_2(PR_2)H]^+$.[11] On the other hand, $[(C_6Me_6)_2Ru_2H_3]^+$ reacts with thiophenols RSH to give, depending on the molar ratio, complexes of the type $[(C_6Me_6)_2Ru_2(SR)H_2]^+$ (R = *p*-C_6H_4−CH_3 for, **1**) and $[(C_6Me_6)_2Ru_2(SR)_2H]^+$ (R = *p*-C_6H_4−CH_3 for **2**), which have been used as building blocks for conjugated organometallic oligomers (Figure 1).[5] The formation of trithiolato-bridged complexes is not observed because of the steric hindrance by the arene ligands.

We decided to take advantage of this specific reactivity to develop a new class of organometallic oligomers by using aromatic dithiols instead of monothiols. Thus, the dinuclear trihydrido complex $[H_3Ru_2(C_6Me_6)_2]^+$reacts in ethanol with one equivalent of HS−C_6H_4−SH or HS−C_6H_4−S−C_6H_4−SH to give the cationic oligomers $[HRu_2(C_6Me_6)_2(S-C_6H_4-S)]_n^{n+}$ (**3**) or $[HRu_2(C_6Me_6)_2(S-C_6H_4-C_6H_4-S)]_n^{n+}$ (**4**), which can be isolated in good yields as the tetrafluoroborate salts (Scheme 1).

Both cationic oligomers **3** and **4**, which are well-soluble in alcohols, acetone, and chlorinated solvents as the tetrafluoroborate salts, have been characterized by NMR spectroscopy (see Experimental Section). The length of oligomers, which is in the range of 4−7 units, has been determined by Maldi-ToF experiments. To the best of our knowledge, **3** and **4** represent the first main chain organometallic oligomers containing dinuclear ruthenium units as building blocks, as most of the published work is on dinuclear molybdenum or tungsten complexes.[12]

The UV−visible spectra of the ruthenium complexes **1** and **2** show a strong band centered at, respectively, 518 nm ($\epsilon \cong 4800$ L mol^{-1} cm^{-1}) and 484 nm ($\epsilon \cong 4200$ L mol^{-1} cm^{-1}). These two bands can be attributed to metal-to-ligand charge transfer (MLCT) transitions (see Table 1). The blue shift in going from **1** to **2** (34 nm) is probably due to strong steric hindrance, which forces the arene substituants to adopt a more titled geometry in **2** than in **1**, observed in the molecular structures of these cations.[5]

Complex **1** exhibits an additional band centered at 367 nm, which can be assigned to a $\pi-\pi^*$ transition of the organic ligand. The corresponding $\pi-\pi^*$ transition band of complex **2** is much weaker (see Figure 2). The UV−visible spectrum of cations of the trithiolato-bridged cation $[(arene)_2Ru_2$-

Scheme 1. Synthesis of Oligomers 3 and 4

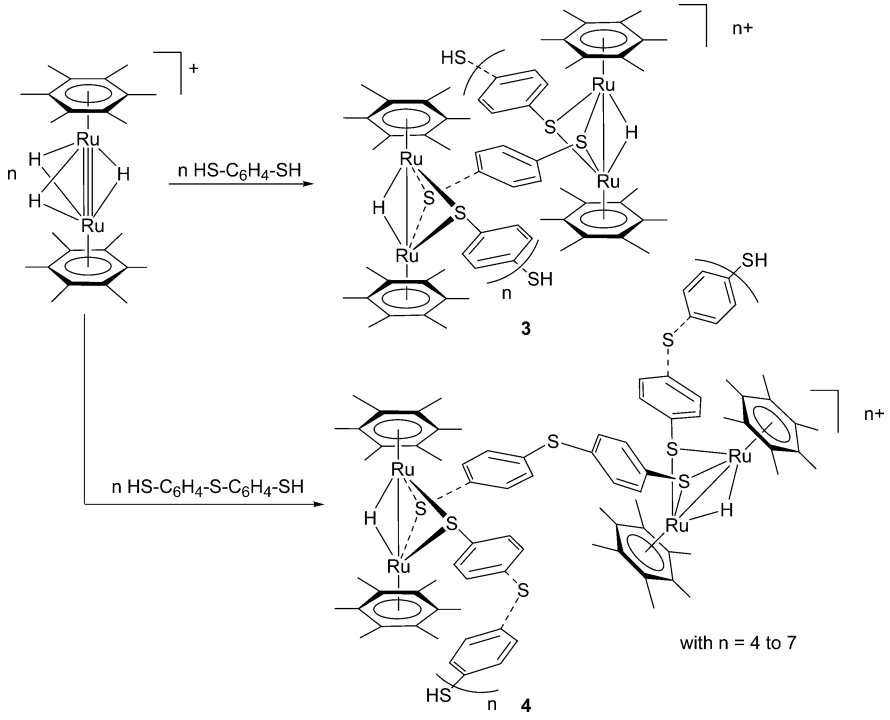

Table 1. Absorption Wavelengths and Molecular Extinction Coefficients of [1][BF_4], [2][BF_4] (conc. 1.7 × 10^{-4} mol·l^{-1}), [3][BF_4] and [4][BF_4] (conc. 1.0 × 10^{-5} mol L^{-1}) in Acetone

compd	λ_1 (nm)/ϵ (L mol^{-1} cm^{-1})	λ_2/ϵ (L mol^{-1} cm^{-1})
1[BF_4]	367/3610	518/4800
2[BF_4]		484/4200
3[BF_4]		481/71700
4[BF_4]		477/20500

$(p\text{-}S{-}C_6H_4{-}CH_3)_3]^+$, exhibits only a $\pi-\pi^*$ transition band centered at 315 nm, but no MLCT absorption,[13] indicating that metal-to-ligand charge transfert decreases with the increasing of the number of thiolato ligands.

The absorption maxima in the UV−visible spectra of oligomers **3** and **4** are very close to those of complex **2**, which contain the same diruthenium dithiolato building block (see Figure 3). However, the molecular extinction coefficients are larger for the two oligomers than for complex **2**. This hyperchromic effect is probably due to the well-ordered structure in the case of the oligomers. The hypochromic effect by going from oligomer **3** to oligomer **4** can be explained by the shorter dithiolato connecting units in **3** (−S−C_6H_4−S−) than in **4** (−S−C_6H_4−S−C_6H_4−S−).

The electrochemical behavior of complexes **1** and **2** and of oligomers **3** and **4** has been studied in acetonitrile solution of the corresponding tetrafluoroborate salts, both in oxidation and in reduction modes.

Oxidation of the Complexes 1 and 2 and Oligomers 3 and 4. In the case of **1**, an irreversible peak potential is visible at 0.184 V for a switch potential of 0.680 V (see Table 2), which can be assigned to the irreversible oxidation of μ_2-thiolato bridges. The variation of the current oxidation as a function of the scan rate is not a straight line, which implies that the process is not a diffusion-controlled process. Moreover, the potential corresponding to the peak current increases with the scan rate. For a higher switch potential, 1.560 V, a second irreversible peak is observed at E_{pA2} = 1.160 V, assigned to the redox couple RuII/RuIII. The potentials found for **1** are close to those observed in chloro arene-ruthenium complexes,[14,15] but higher than those found for complexes of the type bis(2,2′-bipyiridine)-dithiolato-ruthenium.[16]

Complex **2** gives rise to an irreversible oxidation peak at E_{pA1} = 0.300 V, which corresponds to the irreversible oxidation of μ_2-thiolato bridges, and a second peak at 0.742 V, assigned to the redox couple RuII/RuIII. As expected, the RuII/RuIII oxidation peak is found at a lower potential for **2** than for **1**. This could be explained by the stabilization caused by the second toluyl substituent in **2** in comparison with **1**.

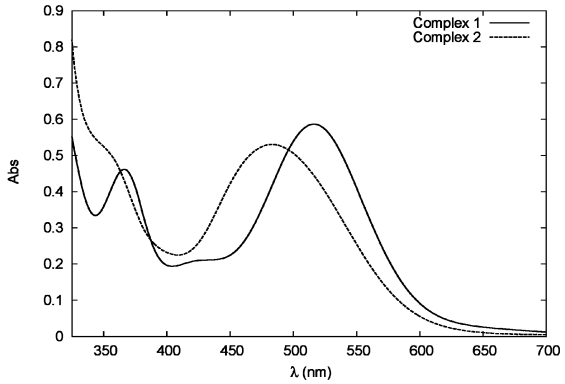

Figure 2. Absorption spectra of complexes [**1**][BF_4] and [**2**][BF_4] in acetone (conc. 1.7 × 10^{-4} mol L^{-1}).

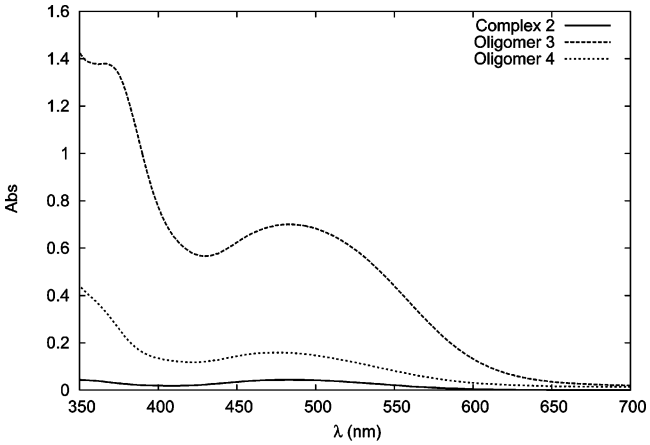

Figure 3. UV-Visible spectra, absorption wavelengths, and molecular extinction coefficients of [**2**][BF_4], [**3**][BF_4], and [**4**][BF_4] in acetone (conc. 1.0 × 10^{-5} mol L^{-1}).

Table 2. Cyclic Voltammetry Data for Oxidation of [1][BF_4], [2][BF_4], [3][BF_4] and [4][BF_4] (conc. 1.1 × 10^{-3} mol L^{-1}) in Acetonitrile (supporting electrolyte, 0.1 mol L^{-1} NBu_4PF_6; on a platinum disc working electrode (reference Fc^+/Fc); scan rate, 100 mV s^{-1})

compd	E_{pA1} (V)	E_{pA2} (V)	E_{pA3} (V)	E_{pC1} (V)
1[BF_4]	0.184	1.160		
2[BF_4]	0.300	0.742		−0.268
3[BF_4]	0.370	0.702		−0.308
4[BF_4]	0.312	0.630	0.990	

For the oligomer **3**, two broad irreversible potentials are obtained at 0.370 and 0.702 V, with the electrochemical characteristics being quite similar to those of complex **2**. The shape of the cyclovoltammogram of oligomer **4** is different in oxidation. Three successive irreversible peaks are visible at 0.312, 0.630, and 0.990 V (see Figure 4). The first peak is due to the irreversible oxidation of the μ_2-thiolato bridges, the second peak is assigned to the oxidation of Ru(II) to Ru(III), and the third peak presumably corresponds to the oxidation of the sulfur atoms linking two aromatic rings, because most organic sulfides display an irreversible peak at a potential higher than 0.7 V versus Fc^+/Fc.[17]

Reduction of the Complexes 1 and 2 and Oligomers 3 and 4. The complexes **1** and **2** exhibit one reversible peak at −1.984 and −2.288 V, respectively, whereas the first

(9) Cassegneau, T.; Mallouk, T. E.; Fendler, J. H. *J. Am. Chem. Soc.* **1998**, *120*, 7848.
(10) (a) Bennett, M. A.; Ennett, J. P.; Gell, K. I. *J. Organomet. Chem.* **1982**, *233*, C17. (b) Jahncke, M.; Meister, G.; Rheinwald, G.; Stoeckli-Evans, H.; Süss-Fink, G. *Organometallics* **1997**, *16*, 1137.
(11) Tschan, M. J.-L.; Chérioux, F.; Karmazin-Brelot, L.; Süss-Fink, G. *Organometallics* **2005**, *24*, 1974.
(12) (a) Cotton, F. A.; Murillo, C. A.; Villagran, D.; Yu, R. *J. Am. Chem. Soc.* **2006**, *128*, 3281. (b) Cotton, F. A.; Lin, C.; Murillo, C. A. *Acc. Chem. Res.* **2001**, *34*, 759.
(13) Chérioux, F.; Therrien, B.; Sadki, S.; Comminges, C.; Süss-Fink, G. *J. Organomet. Chem.* **2005**, *690*, 2365.
(14) Štěpnička, P.; Gyepes, R.; Lavastre, O.; Dixneuf, P. H. *Organometallics* **1997**, *16*, 5089.
(15) Therrien, B.; Vieille-Petit, L.; Jeanneret-Gris, J.; Štěpnička, P.; Süss-Fink, G. *J. Organomet. Chem.* **2004**, *689*, 2456.
(16) Natsuaki, K.; Nakano, M.; Matsubayashi, G.-E.; Arakawa, R. *Inorg. Chim. Acta* **2000**, *299*, 112.

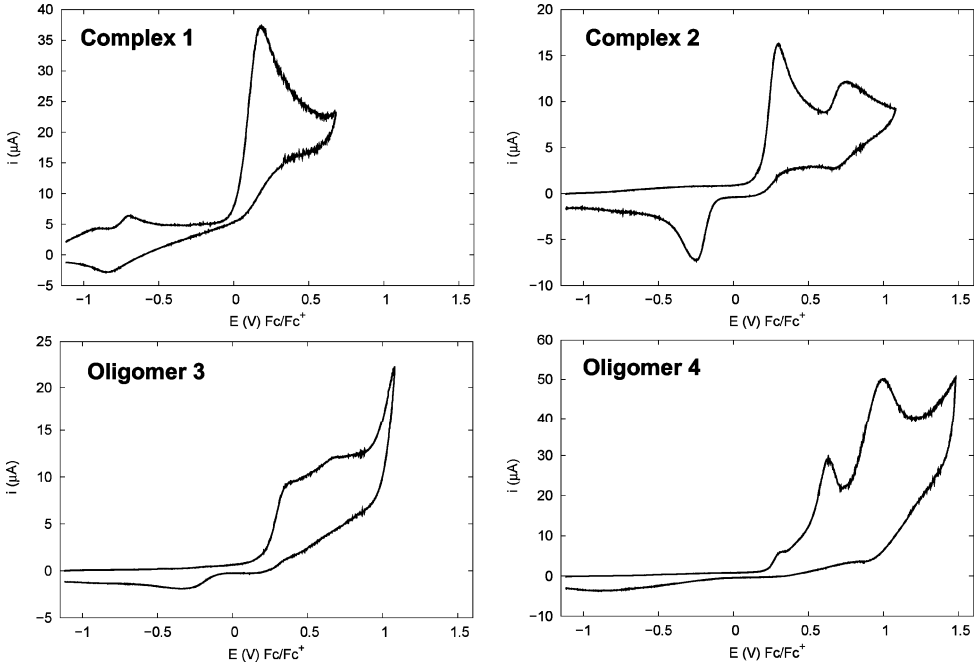

Figure 4. Cyclic voltammograms of [**1**][BF_4], [**2**][BF_4], [**3**][BF_4]. and [**4**][BF_4] (conc. 1.1×10^{-3} mol L^{-1}) in acetonitrile. Supporting electrolyte, 0.1 mol L^{-1} NBu_4PF_6; on a platinum disk working electrode (reference Fc^+/Fc); scan rate, 100 mV s^{-1}.

Table 3. Cyclic Voltammetry Data for Reduction of [1][BF_4], [2][BF_4], [3][BF_4] and [4][BF_4] (conc. 1.1×10^{-3} mol L^{-1}) in Acetonitrile (supporting electrolyte, 0.1 mol L^{-1} NBu_4PF_6; on a platinum disc working electrode (reference Fc^+/Fc); scan rate, 100 mV s^{-1})

compd	E_{pC1}(V)	E_{pC2} (V)	E_{pA1}(V)	E_{pA2} (V)
1[BF_4]	−2.022		−1.946	
2[BF_4]	−2.334		−2.242	−1.142
3[BF_4]	−2.274	−2.546		−1.144
4[BF_4]	−2.274	−3.020		

reduction peak of the oligomers **3** and **4** is irreversible, at a potential E_{pC1} close to −2.27 V (see Table 3). This can be assigned to the reduction of the aromatic ligands, i.e., hexamethylbenzene.[18] Complex **2** and oligomer **3** exhibit an additional irreversible reduction peak close to −1.143 V, which can be assigned to the second reduction of the hexamethylbenzene ligands. The oligomers **3** and **4** give rise to a second reduction peak at −2.546 and −3.020 V, respectively, as shown in Figure 5. In the case of oligomer **3**, the peak at −2.546 V can be assigned to the reduction of the aromatic rings in the main chain of the oligomer. In the case of **4**, the peak at −3.020 V can be attributed to the reduction of the sulfur links between the aromatic rings.[19]

Both the oxidized and reduced forms of complexes **1** and **2** as well as of oligomers **3** and **4** are stable over at least 10 electrochemical cycles, the scan rate varying between 20 and 100 mV s^{-1}. The electrochemical behavior of theoligomers **3** and **4** is set by the electrochemical characteristics of the building blocks, without any differentiation of the individual units.

As the oligomers **3** and **4** are terminated by free thiol functions, we grafted them on a gold electrode. In a simple experimental setup, a gold electrode was immerged for 30 min in a degassed acetonitrile solution of **3** or **4** (20 mL, 1 mM) (see Scheme 2).

The modified electrodes were then washed with an excess of acetonitrile to remove all ungrafted oligomers. The electrochemical behavior of these electrodes was studied in oxidation; the cyclic voltammograms are shown in Figure 6.

The electrode modified with oligomer **3** exhibits an irreversible wave ($E_{1/2}$ = 1.170 V). In the case of oligomer **4** grafted on a gold electrode, two successive reversible peaks are visible at 0.216 and 0.599 V (Figure 6), instead of two irreversible peaks at 0.630 and 0.990 V (see Figure 4). The shift to lower potentials observed in both cases by going from the free oligomers in solution to the electrode-grafted oligomers is a consequence of the redoxactive ruthenium moiety being close to the electrode, thus facilitating the electron transfer.

The oligomers **3** are bound to the gold electrode in rigid positions with a phenyl linker. By comparison with oligomer **3**, oligomer **4** is linked to the gold electrode in a more flexible way because of the sulfur atom between two ruthenium groups. The electron transfer from ruthenium to the electrode should be easier due to this flexibility, which could explain the different half potential ($E_{1/2}$ = 0.804 V) for **4** with respect to that of **3**.

Electrostatic self-assembly (ESA) is a convenient way to deposit a thin-film of organometallic oligomers **3** and **4** on quartz plates, because they are positively charged. First of all, a negative layer must be developed on the quartz substrates. The strategy is based on the grafting of an organosilane with mercapto termination (i.e., dimethoxy-methyl-3-(mercaptopropyl)silane) on the quartz, followed by the oxidation of the mercapto functions to sulfonic acid groups (Scheme 3).[20]

(17) Gregory, I. G.; Tasker, K. M.; Johnson, R. J. K.; Jacob, C.; Peers, C.; Green, K. N. *Chem. Commun.* **2001**, 2490.
(18) Devendra, D. P.; Hutton, A. T.; Hyde, J.; Walkden, A.; White, C. *J. Organomet. Chem.* **2000**, *606*, 188.
(19) Sawyer, D. T.; Sobkowiak, A.; Roberts, J. L. *Electrochemistry for Chemists*, 2nd ed.; John Wiley and Sons: New York, 1994.

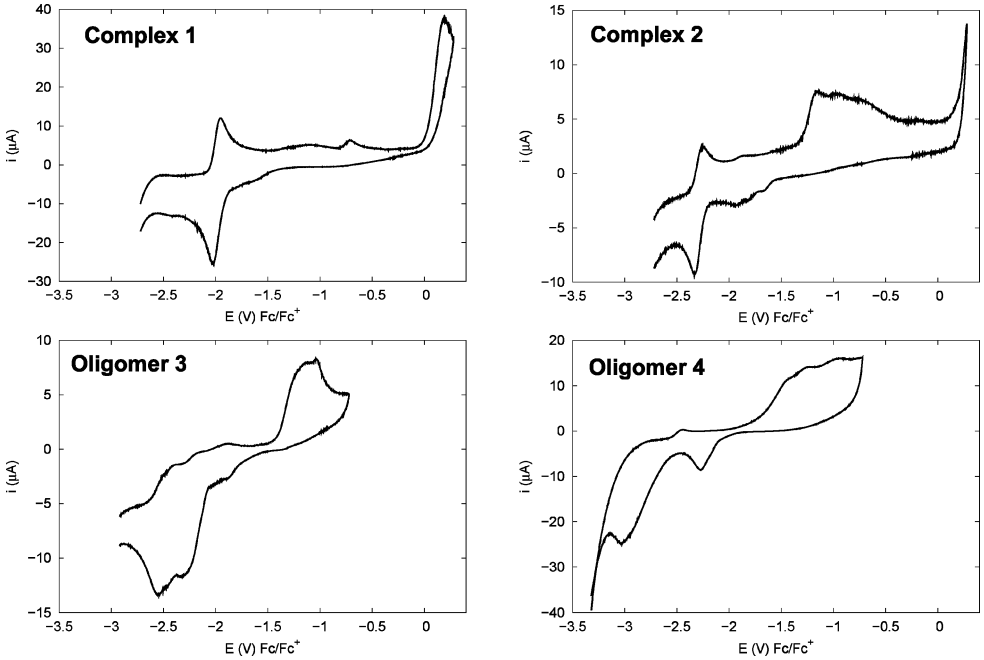

Figure 5. Cyclic voltammograms during the reduction of [**1**][BF_4], [**2**][BF_4], [**3**][BF_4], and [**4**][BF_4] (conc. 1.1×10^{-3} mol L^{-1}) in acetonitrile. Supporting electrolyte, 0.1 mol L^{-1} NBu_4PF_6 on a platinum disc working electrode (reference Fc^+/Fc); scan rate, 100 mV s^{-1}.

Scheme 2. Grafting of Oligomer 3 on a Gold Electrode

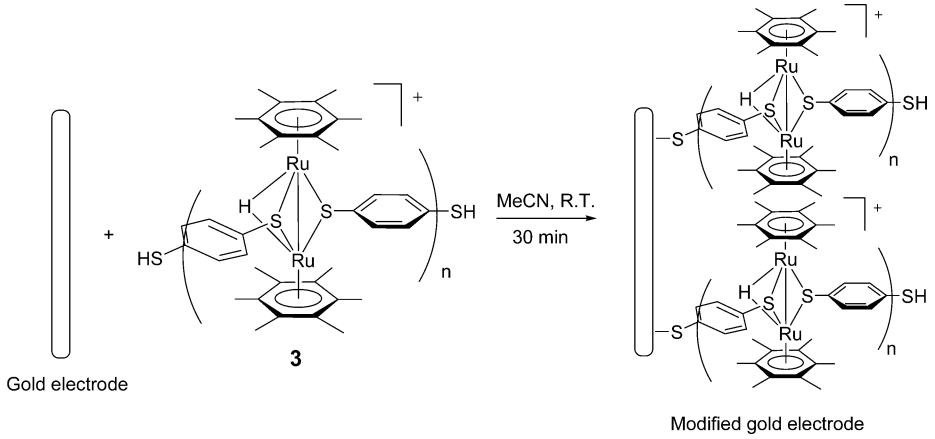

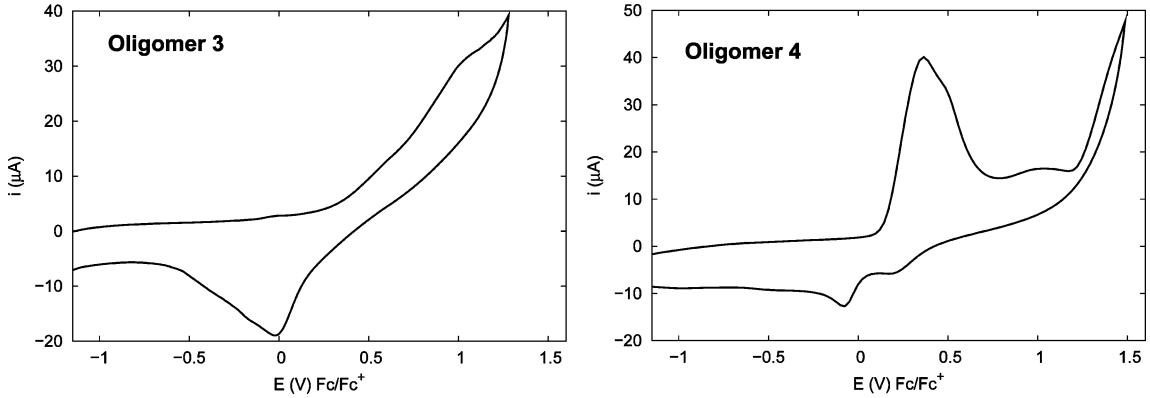

Figure 6. Cyclic voltamograms during the oxidation of [**3**][BF_4] and [**4**][BF_4] grafted on gold electrode in acetonitrile. Supporting electrolyte 0.1 mol L^{-1} NBu_4PF_6; on a platinum disc working electrode (reference Fc^+/Fc); scan rate, 100 mV s^{-1}.

The negative charges are obtained by treatment of sulfonic acid with potassium carbonate in aqueous solution. Electrostatic self-assembly of oligomers **3** and **4** as well as complex **1** and **2** are obtained by immersion of the quartz plates in an acetone solution of the compounds (1 mM) for 1 h. The substrates are then rinsed with large amounts of acetone and dried under a nitrogen stream.

(20) Xiao, Z.; Gu, J.; Hang, D.; Lu, Z.; Wei, Y. *Appl. Surf. Science* **1998**, *125*, 85.

Scheme 3. Grafting of SAMS with Sulfonic Acid Termination on Quartz Substrates

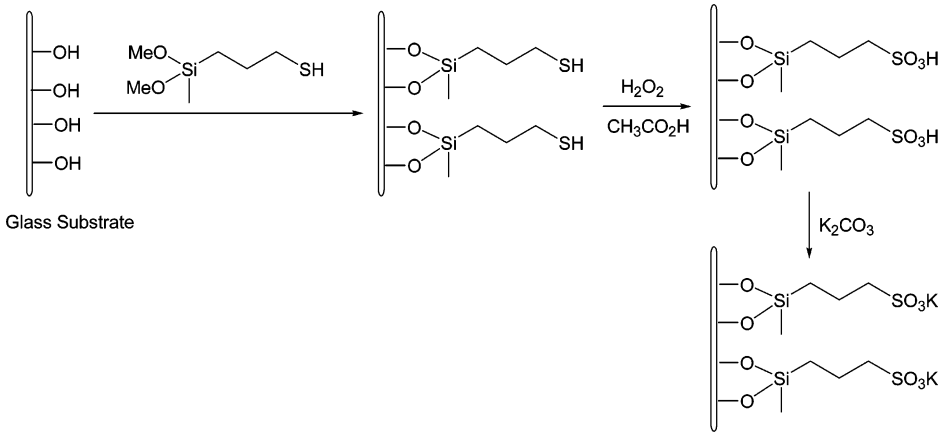

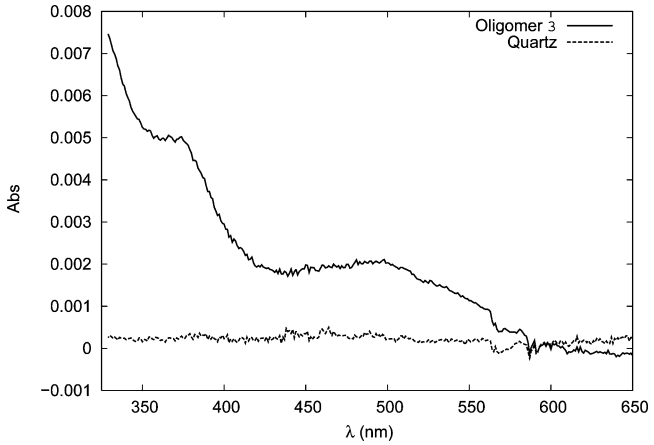

Figure 7. UV−visible spectrum of a self-assembled monolayer of oligomer **3** grafted on a quartz plate.

The absorption maxima of the polymers or the complexes in solution and deposited as a thin film are the same as shown in Figure 7. Repeated measurements every day over a period of 2 weeks show no spectral changes, which means that the ESA of the polymers and the complexes is very stable.

Atomic force microscopy (AFM) allows a detailed analysis of the thin-films obtained by ESA on the quartz substrates. AFM images are obtained in the "tapping-mode", in order to minimize the tip−surface interaction and to avoid the destruction of the thin film in the case of the two oligomers and complex **2**. Figure 8 shows the AFM images of complex **2** deposited on quartz substrates.

The root-mean-square (rms) roughness has been calculated for a $2 \times 2\ \mu m^2$ area. The values are close to 1.4 nm for the two substrates. The surface functionalized with complex **2** appears like a quasi complete film with a large number of small holes. The maximum height of the layer measured by a cross section (in the direction indicated by the arrow) is 3 nm (Figure 8). However, the average value of layer thickness (i.e., 1.5 nm) seems to be in good agreement with the formation of one monolayer of complex **2**.

The pictures obtained in the case of the two oligomers **3** and **4** are very similar (Figure 9), but the surface is quite different from that of complex **2**. The layer is formed by small compact grains, the grain size being homogeneous with

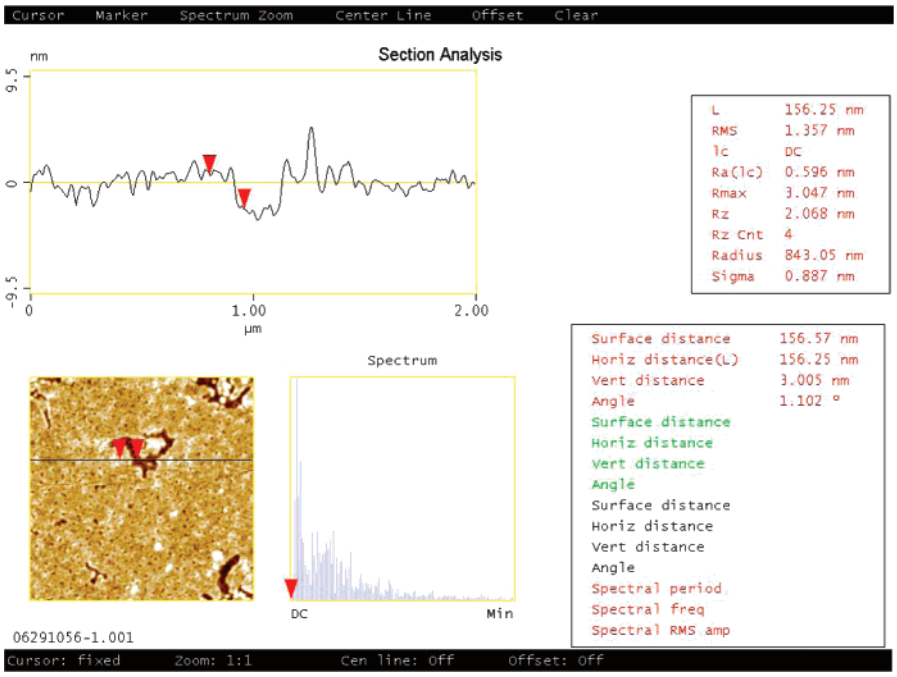

Figure 8. AFM pictures of a self-assembled monolayer of complex **2** grafted on a quartz plate.

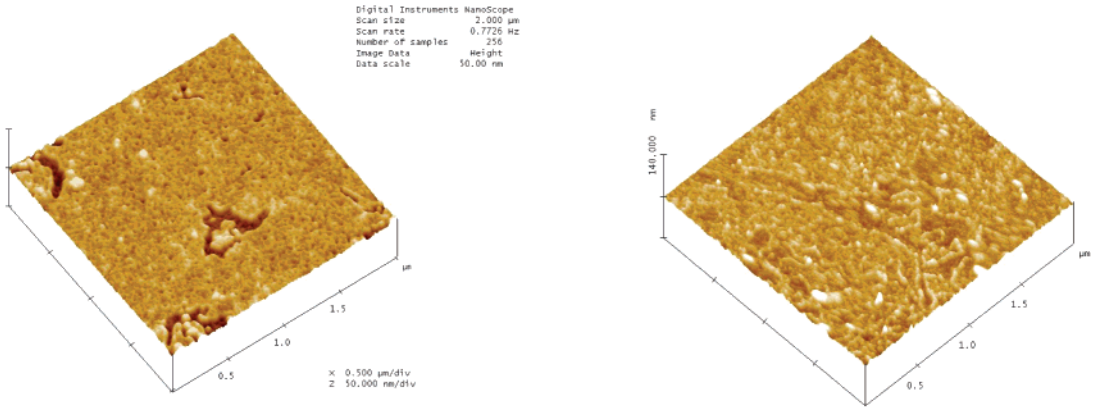

Figure 9. AFM pictures of a self-assembled monolayers of oligomer **3** (left) and of oligomer **4** (right) grafted on a quartz plate.

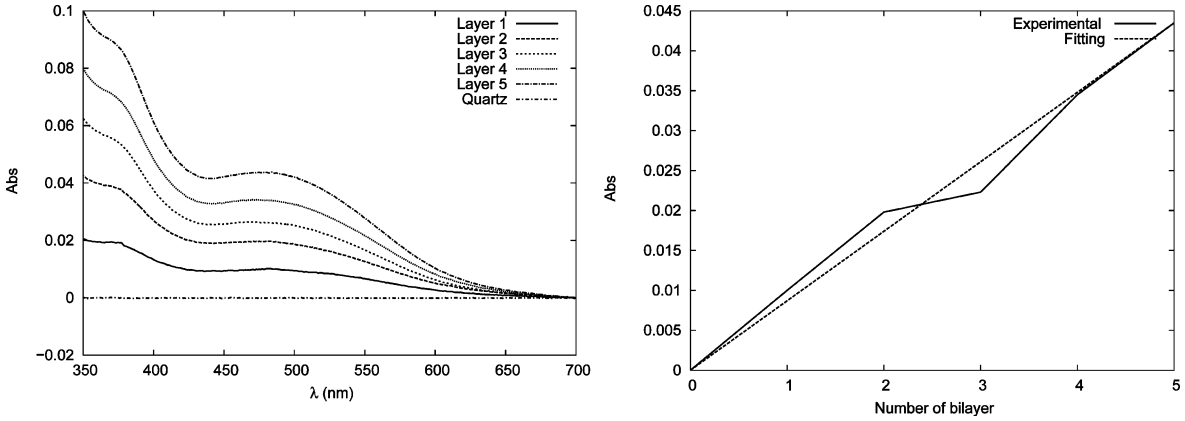

Figure 10. UV−visible spectra of PSS-oligomer **3** superlattices grafted on a quartz plate (left) and variation of the absorption at 481 nm versus the number of PSS-oligomer **3** bilayer (right).

Scheme 4. Layer-by-Layer Self-Assembly of Organic Polymer−Organometallic Oligomer 3

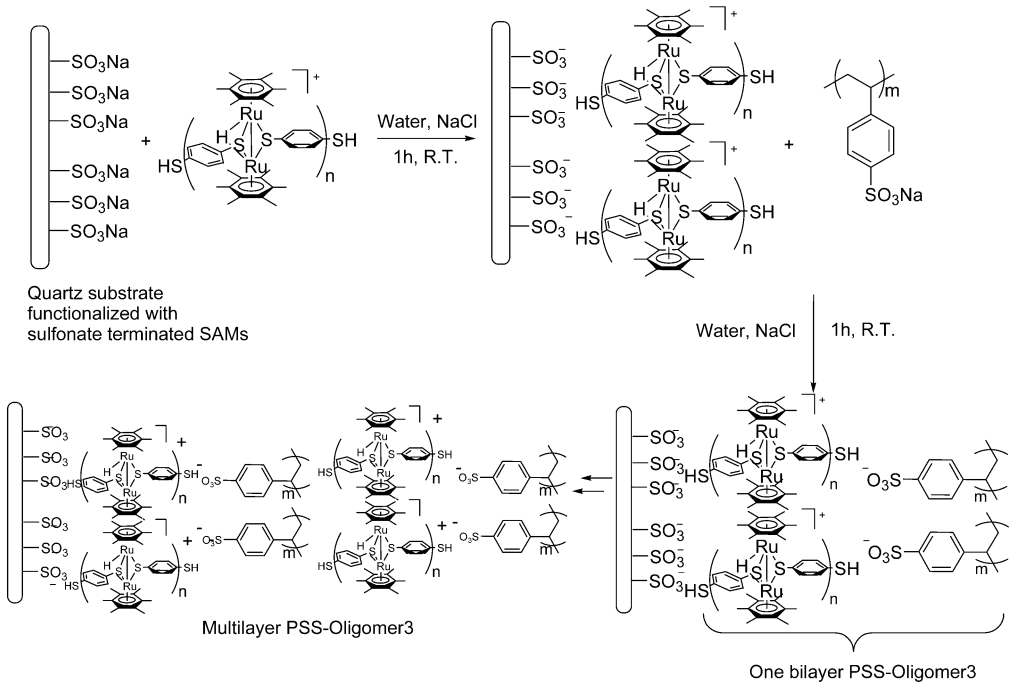

a typical diameter of 30 nm. This morphology can be explained by the formation of nanoconglomerate of the oligomer during its deposition by ESA.

After grafting of the first layer of organometallic oligomers on quartz substrates, we developed a layer-by-layer self-assembly of organic polymer−organometallic oligomer electrostatic superlattices using poly(styrenesulfonate) and oligomers **3** or **4**, as described in Scheme 4. The method consists of depositing a negatively charged layer and a positively charged layer in an alternating fashion.[21]

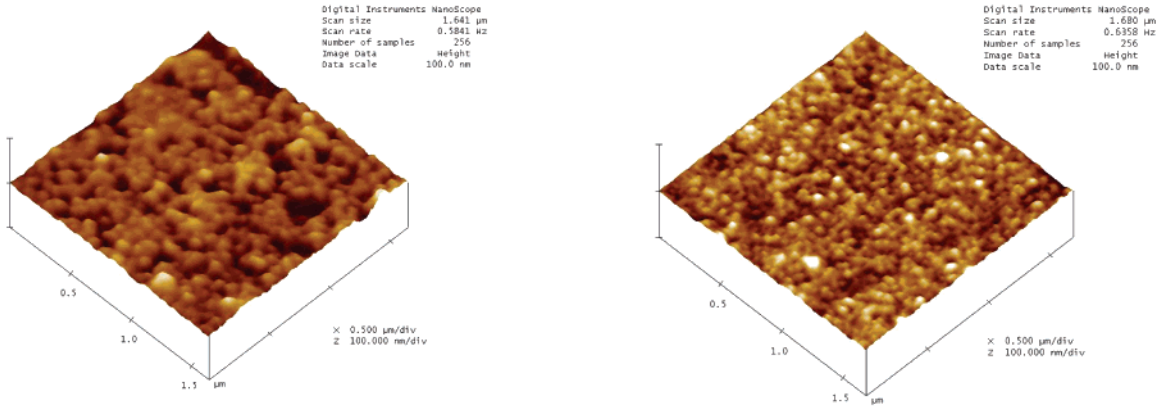

Figure 11. AFM pictures of three layers of PSS-oligomer **3** (left) and of five layers of PSS-oligomer **3** (right) grafted on a quartz plate.

The layer-by-layer assembly of these organic polymer−organometallic oligomer superlattices was monitored using a UV−visible spectrometer (Perkin-Elmer, lambda 900).

Figure 10 shows the absorption change versus the number of deposited PSS-oligomer **3** bilayers. The absorption linearly increased with increasing number of bilayers (right), indicating that the increasing of the thickness of each bilayer is the same at each step.

Atomic force microscopy (AFM) allows a detailed analysis of the multilayers obtained by ESA on the quartz substrates. Figure 11 shows the AFM images of multilayer PSS-oligomer **3** obtained in "tapping-mode" deposited on quartz substrates.

The topological examination of quartz-supported PSS-oligomers **3** multilayers was carried out using AFM. The results demonstrate that the increasing of the number of bilayer induces a smoothing of the surface in accordance with the literature.[22] The multilayer system are well-ordered and more compact than monolayer of oligomer.

Conclusion

We have developed a new type of organometallic oligomers containing dinuclear ruthenium cores connected by sulfur-containing organic links. The optical and electrochemical properties of these oligomers have been studied in comparison with those of the organometallic building blocks. Thin film depositions have successfully been done by electrostatic self-assembly.

Experimental Section

Solvents (puriss., p.a.) were degassed and saturated with nitrogen prior to use. All manipulations were carried out under nitrogen by using standard Schlenk techniques. The dinuclear complex $[(C_6Me_6)_2Ru_2H_3]^+$, isolated as tetrafluoroborate salt, was synthesized as previously described.[10] All reagents were purchased from Aldrich or Fluka and used as received. Silica gel (type G) used for preparative thin-layer chromatography was purchased from Macherey Nagel GmbH. Deuterated NMR solvents were purchased from Cambridge Isotope Laboratories, Inc. NMR spectra were recorded using a Varian-Gemini 200 MHz spectrometer, and ESI mass spectra were recorded at the University of Fribourg by Prof. Titus Jenny. Microanalyses were carried out by the Laboratory of Pharmaceutical Chemistry, University of Geneva. UV−visible spectra have been recorded with a Perkin-Elmer Lambda 900 apparatus. AFM measurements have been performed with NanoscopeIIIa Veeco apparatus.

Synthesis of [3][BF_4] by Reaction of [$(C_6Me_6)_2Ru_2H_3$][BF_4] with HS−Ph−SH. Dibenzenethiol (25.3 mg, 0.179 mmol) was added to a solution of [**1**][BF_4] (100 mg, 0.162 mmol) in degassed puriss. ethanol (50 mL) under nitrogen at room temperature in a Schlenk tube. The resulting solution was refluxed and stirred for 24 h. The reaction mixture was then cooled to room temperature, and the solvent was evaporated to dryness. The crude product was washed 3 times with ether (4 × 50 mL) and then the red solid obtained was dried under a vacuum to give 107 mg of oligomer [**3**][BF_4] (yield 85%).

^{1}H NMR (200 MHz, [D_6]acetone, 25 °C): δ 7.68−7.16 (m, 4H, S-*Ph*-S), 2.26 (m, 36H, $C_6(CH_3)_6$), −11.94 (m, 1H, hydride).

Synthesis of [4][BF_4] by Reaction of [$(C_6Me_6)_2Ru_2H_3$][BF_4] with HS−Ph−S−Ph-SH. 4,4′-Thiobisbenzenethiol (44.7 mg, 0.179 mmol) was added to a solution of [**1**][BF_4] (100 mg, 0.162 mmol) in degassed puriss. ethanol (50 mL) under nitrogen at room temperature in a Schlenk tube. The resulting solution was refluxed and stirred for 24 h. The reaction mixture was then cooled to room temperature, and the solvent was evaporated to dryness. The crude product was washed 3 times with ether (4 × 50 mL) and then the red solid obtained was dried under a vacuum to give 130 mg of [**4**][BF_4] (yield 90%).

^{1}H NMR (200 MHz, [D_6]acetone, 25 °C): δ 7.58−7.06 (m, 8H, S-*Ph*-S-*Ph*-S), 2.23 (m, 30H, $C_6(CH_3)_6$), 1.98 (m, 6H, $C_6(CH_3)_6$), −11.94 (m, 1H, hydride).

Preparation of SAMs on Quartz Substrates. *Cleaning of Glass Wafers.* The glass wafers were sonicated in isopropanol for 45 min and then cleaned with hot piranha solution 1:3 H_2O_2:H_2SO_4 at 90 °C (***Caution****: Piranha solution reacts violently with organic materials and should be handled with extreme care*) for 2 h. The wafers were then rinsed three times with large amounts of deionized water. The water contact angle was controlled for each substrate. The cleaning process was repeated until this angle was below 5°.

Solution-Phase Silanization. Monolayers were prepared by immersion overnight of cleaned wafers in a 100 μM toluene solution (100 mL) of 3-(dimethoxymethylsilyl)-1-propanethiol at room temperature. The wafers were then rinsed with large amounts of toluene and baked for 1 h at 110 °C.

Oxidation of Thiol Terminated SAMs. The oxidation of the thiol groups on the surface to the desired sulfonated monolayer was

(21) Ginzburg, M.; Galloro, J.; Jäkle, F.; Power-Billard, K. N.; Yang, S.; Sokolov, I.; Lam, C.; Neumann, A. W.; Manners, I.; Ozin, G. A. *Langmuir* **2000**, *16*, 9609.
(22) (a) Lvov, Y.; Decher, G.; Möhwald, H. *Langmuir* **1993**, *9*, 481. (b) Kerimo, J.; Adams, D. M.; Barbara, P. F.; Kaschak, D. M.; Mallouk, T. E. *J. Phys. Chem. B* **1998**, *102*, 9451.

carried out by dipping the wafers into the solution of 30% H_2O_2/HOAc for 90 min at 50 °C. The wafers were then washed extensively with chloroform and rinsed with distilled water and finally dried in a nitrogen stream.

Characterization of SAMs. The water contact angle was measured for each substrate, with the values obtained being close to 70 and 30° for HS- and HO_3S-terminated SAMs, respectively.[23]

Preparation of PSS-Oligomer Multilayers by Electrostatic Self-Assembly. Glass substrates are silanized by 3-(dimethoxymethylsilyl)-1-propanethiol and oxidized by H_2O_2/HOAc. The concentrations of the polyelectrolyte solutions were 10 mM polystyrene sulfonate (PSS) and 10 mM oligomer **3** or **4**, on the basis of the respective monomer repeat units. Each solution was made in 0.1 M NaCl and filtered prior to use. Following adhesion of the first charged primer layer, the substrates were alternately placed in the polyanion (PSS) and polycation (oligomers **3** or **4**) solutions for at least 1 h and than washed with water, ultrasonicated for 10 min, and finally dried with a gentle stream of nitrogen.

Electrochemical Measurements. *Free Oligomers in Solution.* Acetonitrile (Aldrich, 99.5%) was distilled over P_2O_5 prior to voltammetric analyses. Cyclic voltammetry experiments were carried out in an acetonitrile solution containing NBu_4PF_6 (0.1 M) in a 20 mL three-necked round-bottom flask cell. The potentiostat used was a PC-controlled EG&GPAR 273 instrument. The working electrode was a platinum disk with a 0.785 mm^2 area. The counter electrode was a platinum wire, and the reference electrode was a silver wire. The reference was calibrated after each experiment against the ferrocene/ferrocenium couple ($E^0_{Fc/Fc^+} = 0.72$ V vs the Ag reference). The potentials first determined vs the Ag pseudo-reference electrode were then calibrated using ferrocene/ferrocenium (Fc/Fc^+) in the same electrolytic solution as recommended by IUPAC.[24] The precision of the measurements was about ±5 mV. All experiments were carried out in a glove box under Ar gas.

Modified Gold Electrodes. Gold electrodes with a geometrical surface of 0.785 mm^2 were polished well with Mecaprex diamond compound (10 μm). The polished electrodes were electrochemically cleaned by cyclic voltamperometry between −0.5 and 1.8 V at a scan rate of 100 mV s^{-1}. The pretreated electrode was immersed in a solution of oligomers **3** or **4** (concentration of 1.093×10^{-3} M in acetonitrile, NBu_4PF_6 0.1 M) for a period of 30 min. Both modified electrode was washed with a solution of acetonitrile.

Acknowledgment. We thank the Johnson Matthey Technology Centre for a generous loan of ruthenium chloride and the Swiss National Science Foundation and University of Franche-Comté for grants.

CM070908P

(23) Balachander, N.; Sukenik, C. N. *Langmuir* **1990**, *6*, 1621.
(24) Gritzner, G.; Kuta, G. J. *Pure Appl. Chem.* **1984**, *56*, 461.